Supporting Information

Mixed-Linker Strategy in Covalent Organic Frameworks for Enhanced Sunlight-Driven Photocatalytic Oxidation Activity and Stability

Jikuan Qiu,*[a] Xinchun Xue,[a] Kangna Zhang,[a] Xiaoxin Tian,[a,b] Wenrui Wan,[a] Tingting Fan,[a] Zhiyong Li,[a] Huiyong Wang,[a] Yuling Zhao*[a]

[a]School of Chemistry and Chemical Engineering, Key Laboratory of Green Chemical Media and Reactions, Ministry of Education Henan Normal University, 46 Jianshe Road E., Xinxiang, 453007, P. R. China

E-mail: qiujikuan@htu.edu.cn; ylzhao@htu.edu.cn

[b]School of Chemistry and Materials Engineering, Xinxiang University, Xinxiang, Henan, 453003, P. R. China

Section S1. Materials synthesis and characterization

Materials

A series of phenylboronic acid (99%) and its derivatives were purchased were from Adamas Reagent (Shanghai, China). The building blocks such as p-phenylenediamine (98%), triphenyl-benzaldehyde (98%), and trialdehyde-triphenylphenol (98%) were purchased from Adamas Reagent (Shanghai, China). Acetic acid (99.7 %), anhydrous acetonitrile (CH_3CN) (≥ 99 %, AR), tetrahydrofuran (THF) (≥ 99%, AR), anhydrous EtOH (≥ 99.5%), and acetone (≥ 99.5%) were purchased from commercially and used without further purification.

Synthesis of TfbPa-COF

Typically, triphenyl-benzaldehyde (Tfb, 0.3 mmol), p-phenylenediamine (Pa, 0.45 mmol), dioxane (1.5 mL), and 1,3,5-trimethylbenzene (1.5 mL) were charged into a glass tube. After dispersing evenly, 3 M acetic acid (0.5 mL) was added, followed by the degassing procedure using freeze-pump-thaw cycles for three times. The glass vial was then flame-sealed and the mixture was allowed to react at 120 °C for 3 days. After being collected by filtration, the precipitate was washed with ethanol, tetrahydrofuran, and acetone. Finally, the solid was dried at under vacuum at 60 °C for 12 h to obtain TfbPa-COF as yellow powder.

Synthesis of TpPa-COF

Typically, trialdehyde-triphenylphenol (Tp, 0.3 mmol), p-phenylenediamine (Pa, 0.45 mmol), dioxane (1.5 mL), and 1,3,5-trimethylbenzene (1.5 mL) were charged into a glass tube. After dispersing evenly, 3 M acetic acid (0.5 mL) was added, followed by the degassing procedure using freeze-pump-thaw cycles for three times. The glass vial was then flame-sealed and the mixture was allowed to react at 120 °C for 3 days. After being collected by filtration, the precipitate was washed with ethanol, tetrahydrofuran, and acetone. Finally, the solid was dried at under vacuum at 60 °C for 12 h to obtain TpPa-COF as brick-red powder.

Synthesis of TpTfbPa-COF

Typically, triphenyl-benzaldehyde (Tfb, 0.15 mmol), trialdehyde-triphenylphenol (Tp, 0.15 mmol), p-phenylenediamine (Pa, 0.45 mmol), dioxane (1.5 mL), and 1,3,5-trimethylbenzene (1.5 mL) were charged into a glass tube. After dispersing evenly, 3 M acetic acid (0.5 mL) was added, followed by the degassing procedure using freeze-pump-thaw cycles for three times. The glass vial was then flame-sealed and the mixture was allowed to react at 120 °C for 3 days. After being collected by filtration, the precipitate was washed with ethanol, tetrahydrofuran, and acetone. Finally, the solid was dried at under vacuum at 60 °C for 12 h to obtain TpTfbPa-COF as orange powder.

Characterization

Power X-ray diffraction (PXRD) data were obtained with an X' Pert3 powder diffractometer at 40 kV and 40 mA with Cu Kradiation from $2\theta = 2°$ to 40° in 0.05° increment. Fourier transform infrared (FT-IR) spectra of the samples were collected on a Spectrum 400 spectrometer (Perkin-Elmer). All samples were ground into a powder with KBr and pelletized before the measurements. Nitrogen adsorption and desorption isotherms were measured at 77 K using an ASiQwin Quantachrome instrument. The samples were treated at 120 °C for 8 h before measurements. Specific surface areas were calculated from the adsorption data using Brunauer-Emmett-Teller (BET) methods. Pore size distribution data were calculated based on the nonlocal density functional theory (NLDFT) model. The morphology of the sample was characterized on a field emission scanning electron microscope (FESEM, Hitachi SU8010) and a transmission electron microscope (TEM, JEM-2100). ^{1}H nuclear magnetic resonance (^{1}H NMR) spectra were recorded by a Bruker Advance III 400 MHz NMR spectrometer with chemical shift in ppm. Solid state magic angle spinning ^{13}C CP/MAS NMR measurement was carried out on a Bruker Avance 400 model 400 MHz NMR spectrometer at a MAS rate of 10 kHz. The X-ray photoelectron spectrum (XPS) was recorded on a Thermo Scientific K-Alpha electron energy spectrometer using Al Kα (1486.6 eV) radiation as the X-ray excitation source. UV-vis spectra were collected on a Shimadzu Corporation UV-2600 220V CH spectrometer. Photoluminescence and Time-resolved PL decay spectra were collected on a Horiba FluoroLog-3 in air atmosphere. ESR spectra were recorded on an EMXplus. Thermal gravimetric analysis (TGA) data were collected on a STA449C thermal analyzer under N_2 atmosphere at a heating rate of 10 ºC min^{-1} within a temperature range of 30-800 °C.

Electrochemical Characterization

Photoelectrochemical and electrochemical measurements including photocurrent, electrochemical impedance spectra (EIS), and Mott-Schottky plot were performed with an electrochemical working station (CHI 760E) via a three-electrode quartz cell. Ag/AgCl electrode and Pt mesh were immersed in aqueous sodium sulfate solution (0.5 M) to serve as the reference electrode and the counter electrode, respectively. The working electrode was prepared as follows: COF material (2 mg) was dispersed in a mixed solution of ethanol (0.2 mL) and Nafion (5 μL) to form a homogeneous slurry. Subsequently, 200 μL of the slurry was transferred and coated on an ITO glass plate (0.5 cm × 0.5 cm), and then dried at 60 °C. For photocurrent measurements, irradiation conditions were the same as photocatalytic tests. In the EIS measurements, the frequency limit was set in the range from 100 kHz to 0.01 Hz with 5 mV of voltage amplitude at the open-circuit potential. For Mott-Schottky plot measurements, the samples were tested with different frequencies at 500, 1000, and 1500 Hz.

Section S2. Photocatalytic procedures

General procedure for photocatalytic oxidation of phenylboronic acid

A 10 mL Schlenk tube equipped with a stir bar, was loaded with the mixture of *phenylboronic acid* (0.25 mmol), COF (5 mg), N. N-Dimethylethylamine (DIPEA, 1.25 mmol) and CH_3CN (2 mL). The reaction mixture underwent irradiation in a photo-reactor equipped with 20 W white LEDs, along with a cooling fan, for duration of 4 hours under an air atmosphere. Upon completion of the reaction, the photocatalyst was collected by centrifugation, and the solvent was concentrated under reduced pressure. The resulting residue was subjected to purification via flash chromatography on silica gel using a petroleum ether/ethyl acetate mixture as the eluent, leading to the isolation of the desired product.

Recyclability of catalysts

For the recyclability test, the catalysts were separated from the reaction mixtures by centrifugation and washed with THF for three times. After dried at 80 ^{o}C in an oven, the catalysts were reused for the next run under the optimum reaction conditions.

Section S3. Computational details

The crystalline structures of COFs were determined using the density-functional tight-binding (DFTB+) method including Lennard-Jones (LJ) dispersion. The calculations were carried out with the DFTB+ program package[1] version 1.2. DFTB is an approximate density functional theory method based on the tight binding approach and utilizes an optimized minimal LCAO Slater-type all-valence basis set in combination with a two-center approximation for Hamiltonian matrix elements. The Coulombic interaction between partial atomic charges was determined using the self-consistent charge (SCC) formalism.The lattice dimensions were optimized simultaneously with the geometry. Standard DFTB parameters for X-Y element pair (X, Y = C, H, N, and O) interactions were employed from the mio-0-1 set http://www.dftb.org. The interlayer-stacking distances, and crystalstacking energies per monolayer of TpTfbPa-CO COF structure are shown in Supplementary Table S1. The XRD pattern simulation was performed in the reflex software package for crystal determination from PXRD pattern, implemented in MS modeling (Accelrys Inc.). We performed Pawley refinement to optimize the lattice parameters iteratively until the R_P and R_{WP} values converge. The pseudo-Voigt profile function was used for whole profile fitting and Berrar-Baldinozzi function was used for asymmetry correction during the refinement processes.

[1] B. Aradi, B. Hourahine, T. Frauenheim, DFTB+ , a sparse matrix-based implementation of the DFTB method. *J. Phys. Chem. A* , 2007, **111**, 5678-5684.

Section S4. Figures S1-S38

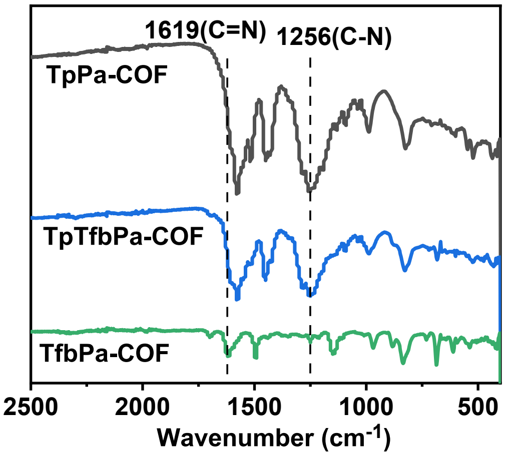

Figure S1 FT-IR spectra of the synthesized COFs.

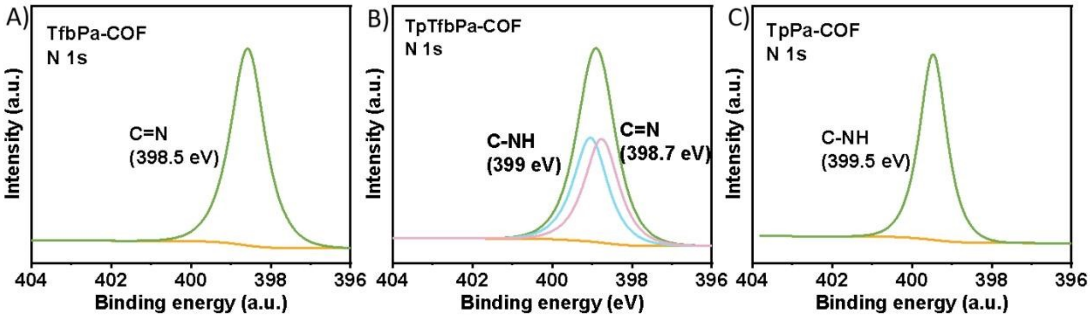

Figure S2 (A-C) N1s XPS spectrum of TfbPa-COF, TpTfbPa-COF and TpPa-COF, respectively. In Figure S2B, the corresponding binding energy of 399.0 and 398.7 eV are assigned to C-N of β-ketoenamine and C-N of imine linkage, respectively. The ratio of Tp to Tfb in the framework of TpTfbPa-COF, calculated from their peak areas, is 1:1.

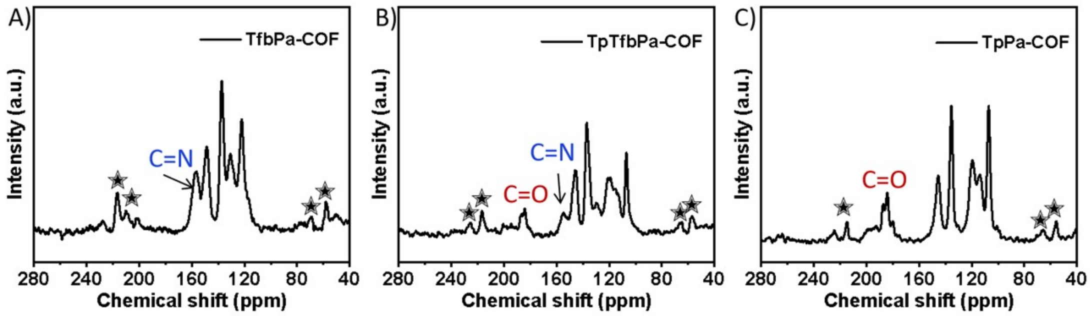

Figure S3 (A-C) ^{13}C CP-MAS NMR spectra and carbon signal assignment of TfbPa-COF, TpTfbPa-COF and TpPa-COF, respectively, the asterisks denote the spinning sidebands. The typical signal at ~156 ppm in the NMR spectrum of TfbPa-COF, TpTfbPa-COF confirmed the formation of a C=N carbon. The typical signal at ~185 ppm in the NMR spectrum of TfbPa-COF, TpPa-COF confirmed the formation of a C=O carbon.

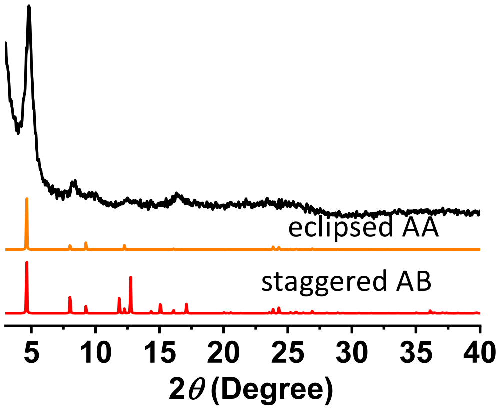

Figure S4 Simulated and experimental PXRD patterns of TfbPa-COF.

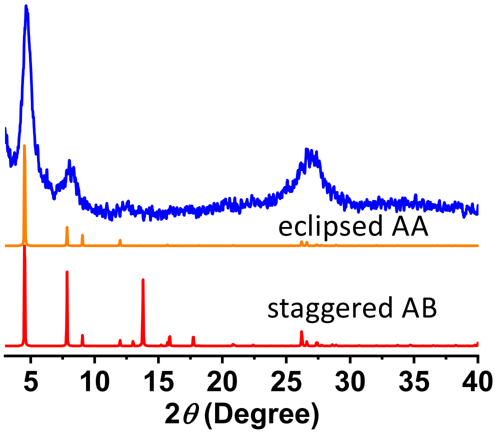

Figure S5 Simulated and experimental PXRD patterns of TpPa-COF.

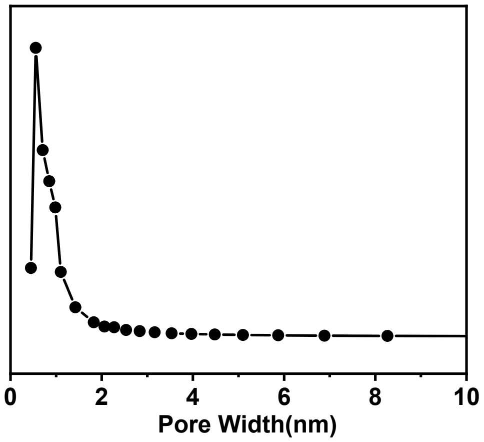

Figure S6 DFT pore size distribution of TpTfbPa-COF.

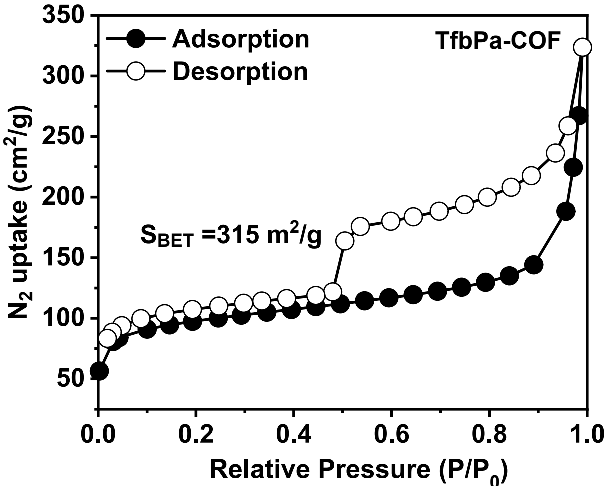

Figure S7 N_2 sorption isotherms of TfbPa-COF

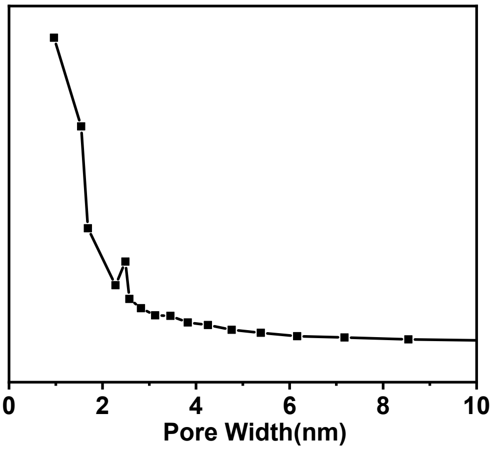

Figure S8 DFT pore size distribution of TfbPa-COF.

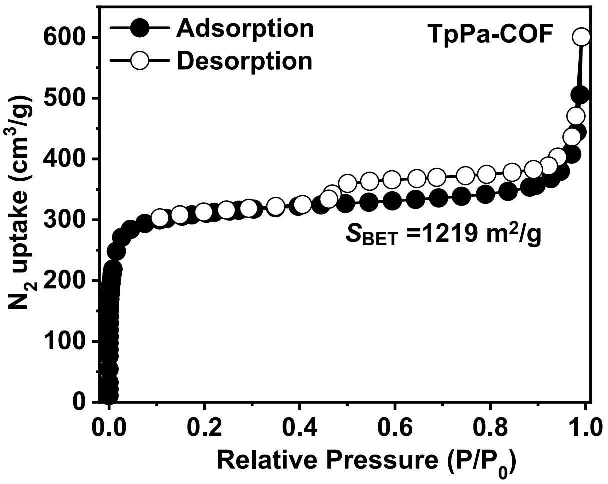

Figure S9 N_2 sorption isotherms of TpPa-COF.

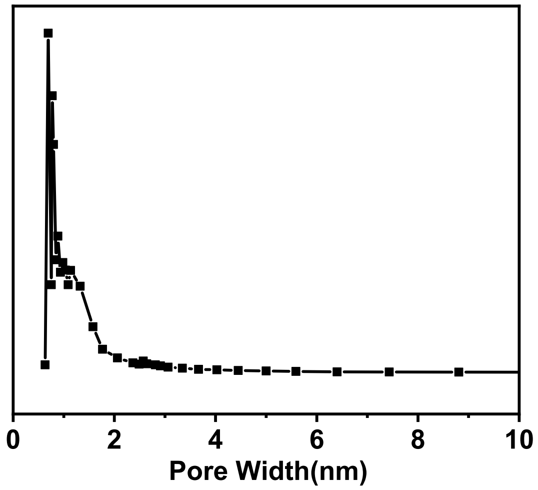

Figure S10 DFT pore size distribution of TpPa-COF.

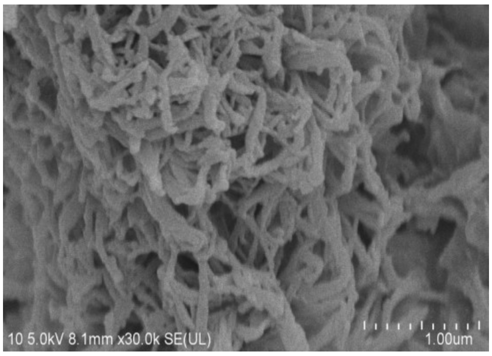

Figure S11 SEM image of TpTfbPa-COF.

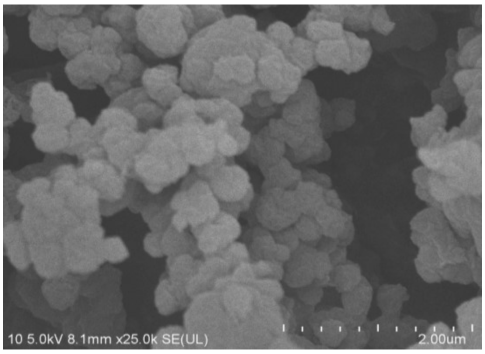

Figure S12 SEM image of TfbPa-COF.

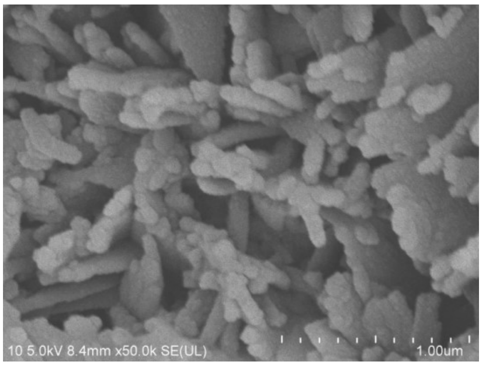

Figure S13 SEM image of TpPa-COF.

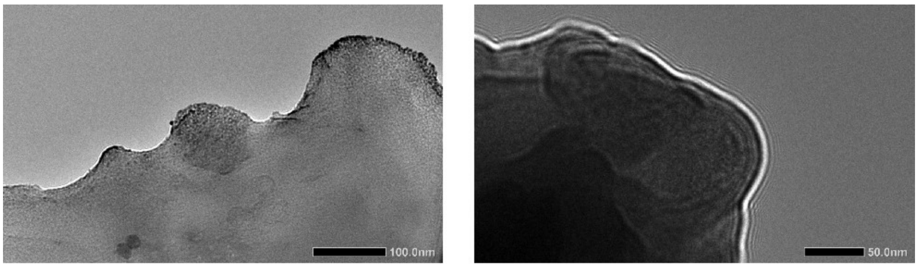

Figure S14 TEM images of TfbPa-COF.

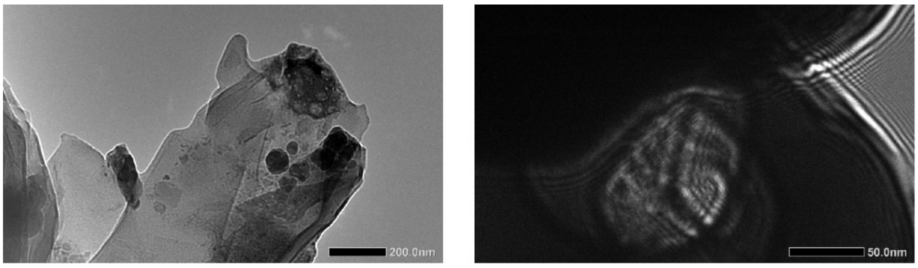

Figure S15 TEM images of TpTfbPa-COF.

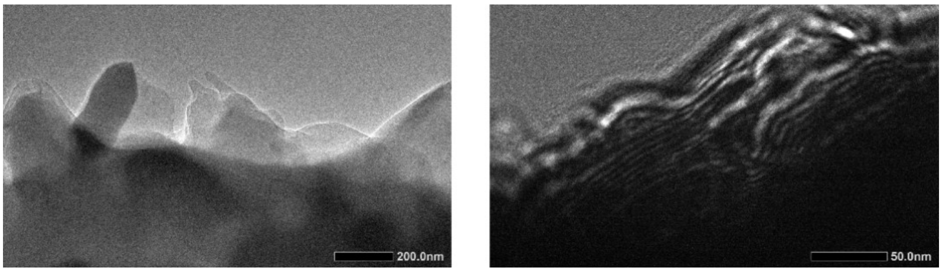

Figure S16 TEM images of TpPa-COF.

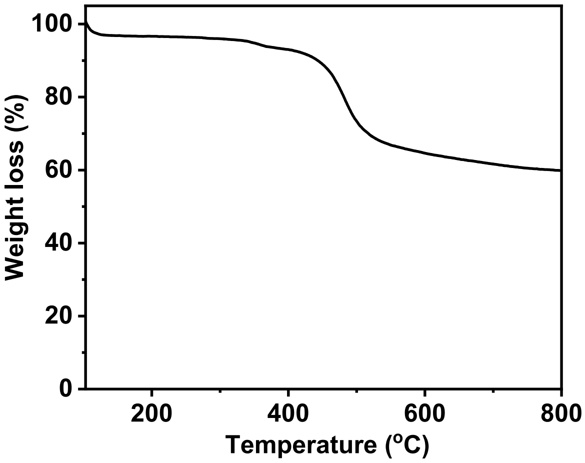

Figure S17 Thermogravimetric curve of TfbPa-COF under N_2.

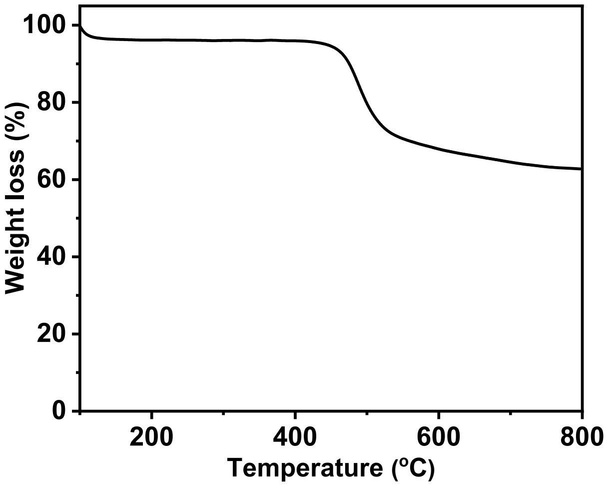

Figure S18 Thermogravimetric curve of TpTfbPa-COF under N_2.

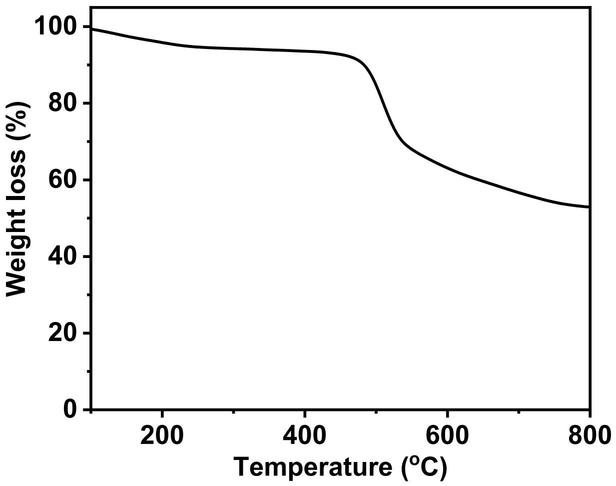

Figure S19 Thermogravimetric curve of TpPa-COF under N_2.

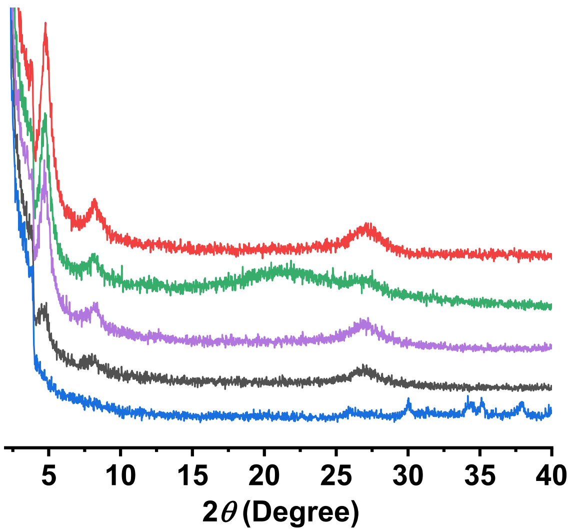

Figure S20 PXRD patterns of samples of TfbPa-COF immersed in, respectively, THF, DMF, boiling water, 3 M HCl, and 3 M NaOH.

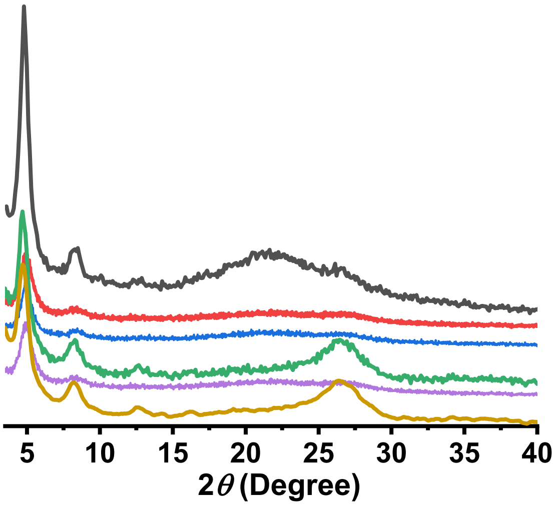

Figure S21 PXRD patterns of samples of TpTfbPa-COF immersed in, respectively, THF, DMF, boiling water, 3 M HCl, and 3 M NaOH.

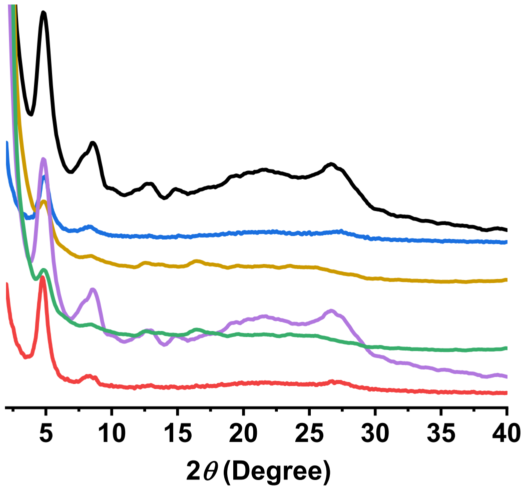

Figure S22 PXRD patterns of samples of TpPa-COF immersed in, respectively, THF, DMF, boiling water, 3 M HCl, and 3 M NaOH.

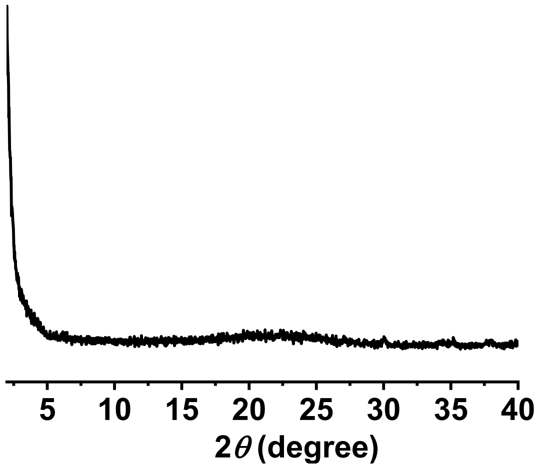

Figure S23. PXRD pattern of TpTfbPa-COF recovered from the reaction. It was noted that the mass of TpTfbPa-COF decreased from 100% to 23% when the reaction finished.

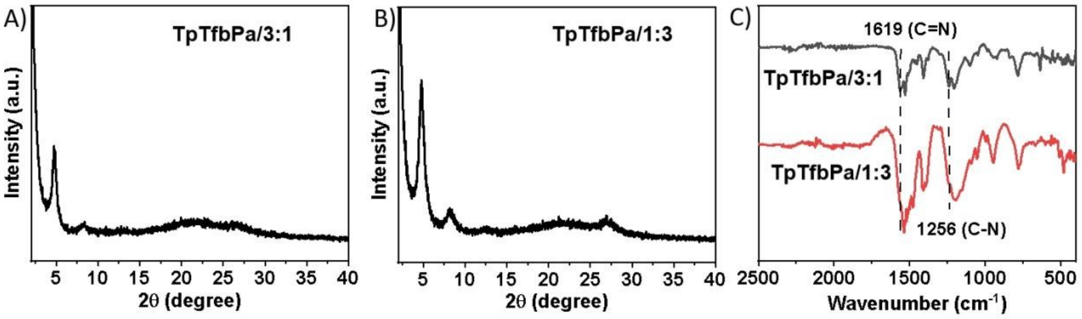

Figure S24 (A, B) The PXRD patterns of samples; c) The FT-IR spectra of samples.

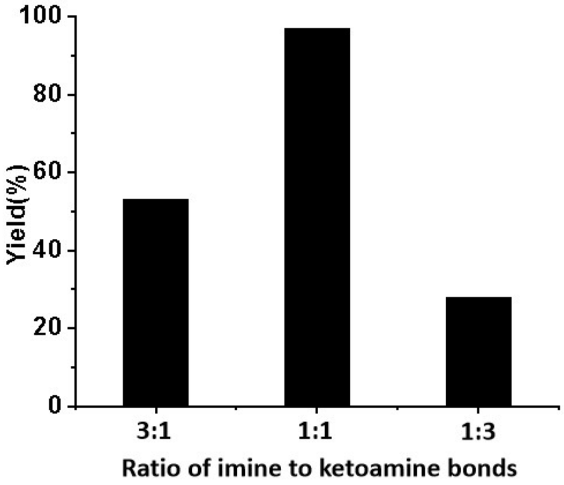

Figure S25 The photocatalytic activity of COFs with different mixed ratios of imine to ketoamine bonds in the oxidation of phenylboronic acid to phenol.

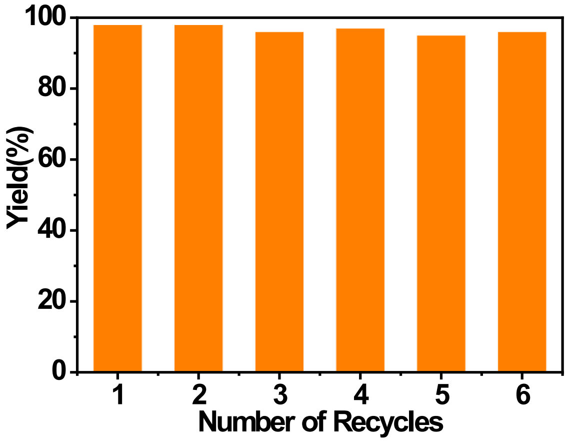

Figure S26 Recyclability of TpTfbPa-COF.

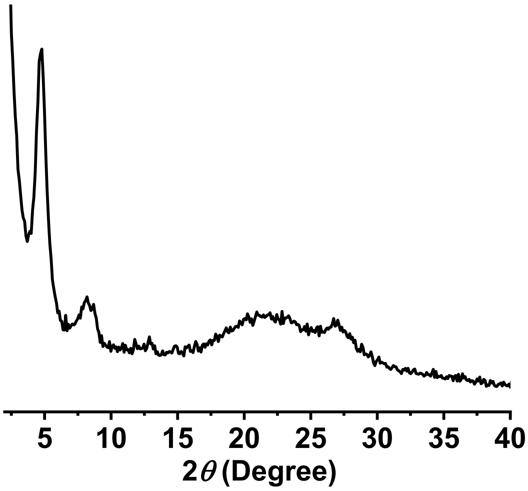

Figure S27 PXRD pattern of TpTfbPa-COF after reused 6 runs.

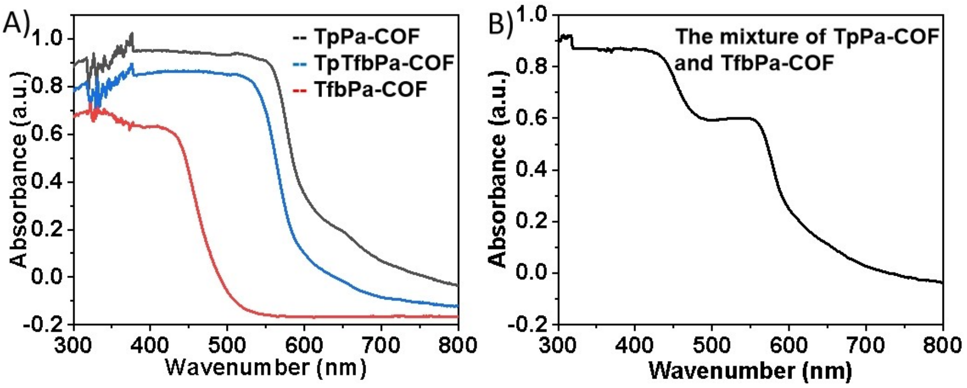

Figure S28 (A) UV−visible diffuse reflectance spectra of TpTfbPa-COF, TpPa-COF and TfbPa-COF. (B) UV−visible diffuse reflectance spectra of the sample of a physical mixture of TfbPa-COF and TpPa-COF. Compared with TpTfbPa-COF, the sample of a physical mixture of TfbPa-COF and TpPa-COF has two distinct light adsorption behaviour (Figure SxB), which are composed of the adsorption spectra of TpPa-COF and TfbPa-COF. Therefore, TpTfbPa-COF has been successfully synthesized by the mixed-linked strategy, rather than a physical mixture of TfbPa-COF and TpPa-COF.

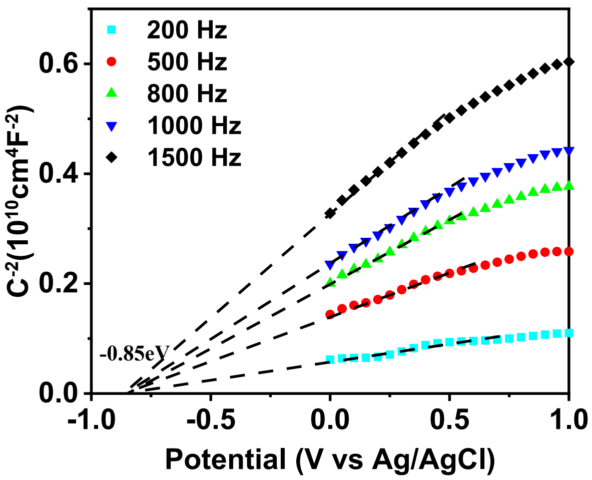

Figure S29 Mott-Schottky curves of TfbPa-COF.

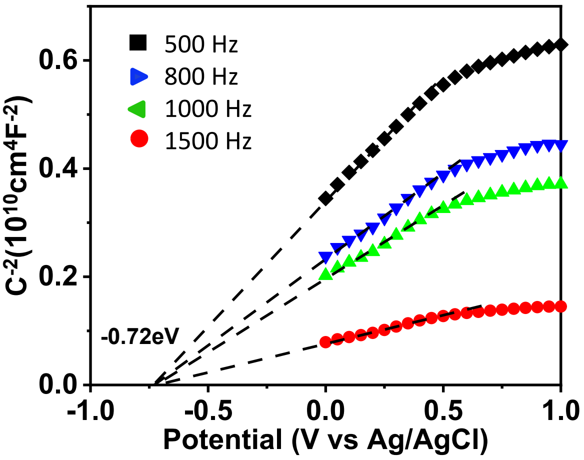

Figure S30 Mott-Schottky curves of TpTfbPa-COF.

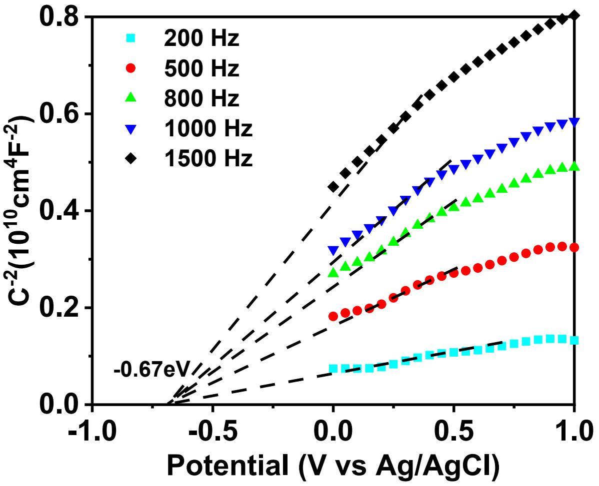

Figure S31 Mott-Schottky curves of TpPa-COF.

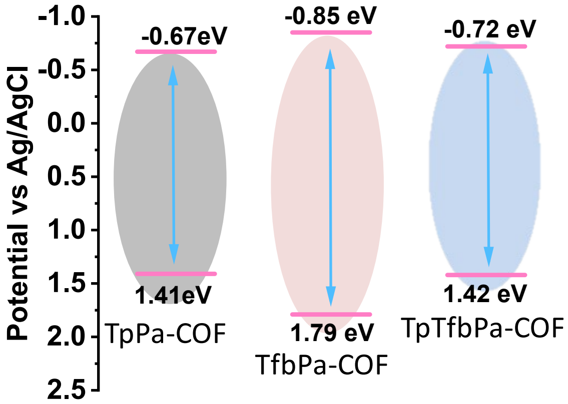

Figure S32 Band positions of TfbPa-COF, TpTfbPa-COF, and TpPa-COF.

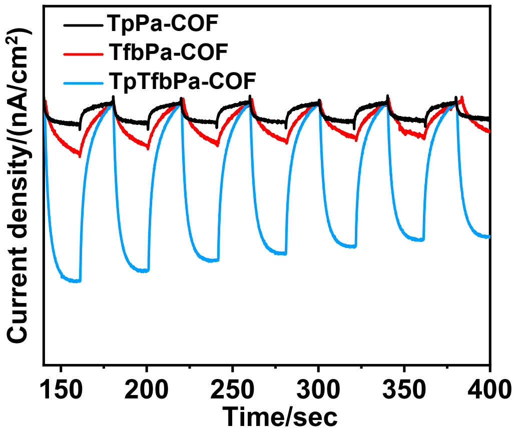

Figure S33 transient photocurrent responses of TpTfb-COF, TfbPa-COF and TpPa-COF.

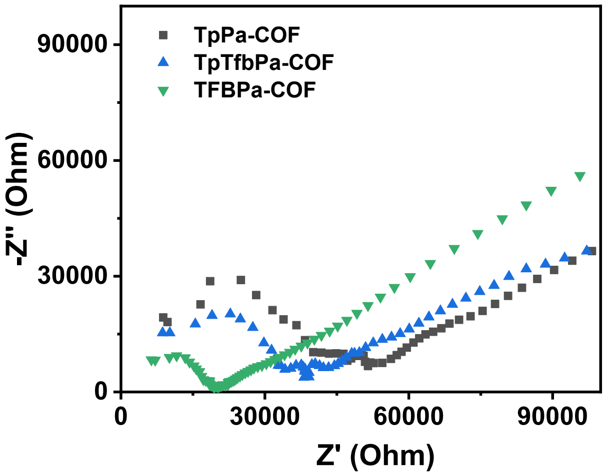

Figure S34 EIS plots of TpTfb-COF, TfbPa-COF and TpPa-COF.

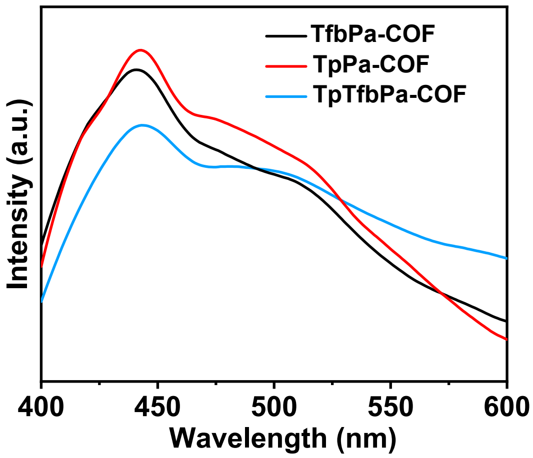

Figure S35 Steady-state photoluminescence (PL) spectra of TpTfb-COF, TfbPa-COF and TpPa-COF.

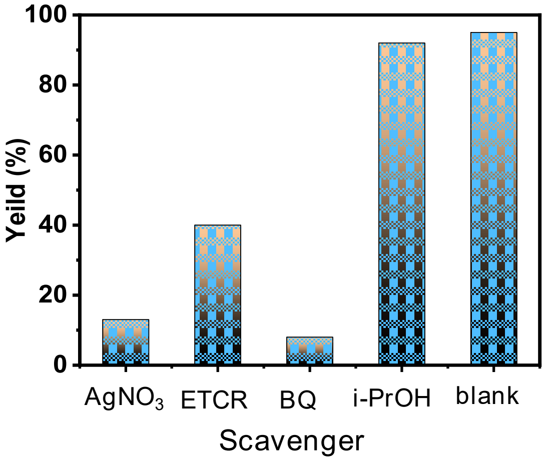

Figure S36 Quenching experiments of photocatalytic oxidation of phenylboronic acid over TpTfbPa-COF.

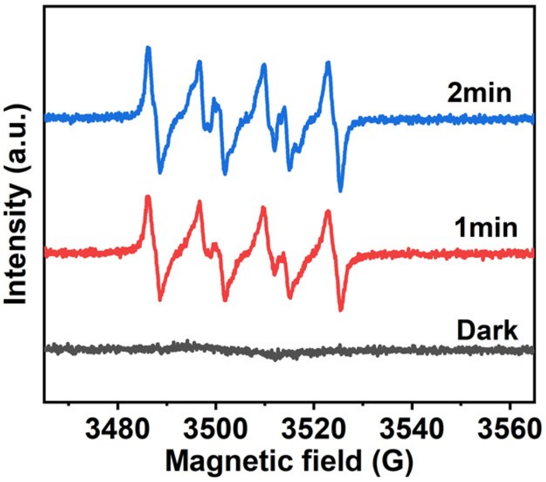

Figure S37 EPR spectra of TpTfbPa-COF in the presence of 5,5-dimethyl-1- pyrroline-Noxide (DMPO), in O_2 atmosphere with 1 min of irradiation, and with 2 min of irradiation.

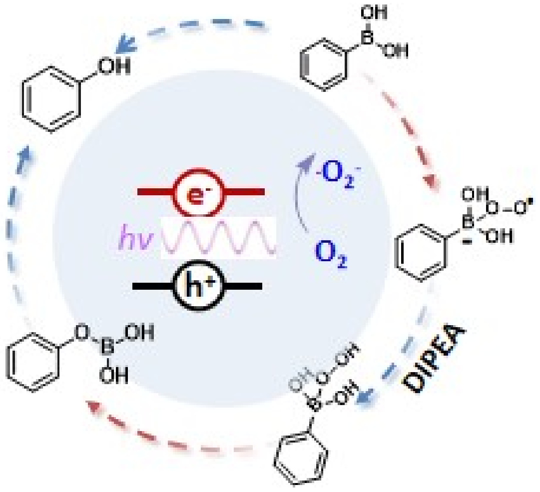

Figure S38 Proposed mechanism of photocatalytic oxidation of phenylboronic acid over TpTfbPa-COF under visible light.

Based on experimental results and previous research reports,[1,2] we propose the following reaction mechanism for the photocatalytic oxidation of phenylboronic acid (Figure 5F). Upon absorption of photons with energy equal to or less than their bandgap, electrons in the covalent organic frameworks are excited to a higher energy state *COF. The excited *COF reduces atmospheric oxygen to form superoxide radicals. Subsequently, these superoxide radicals attack the boron atom of phenylboronic acid, generating peroxide radical intermediate A. Intermediate A then abstracts a hydrogen radical from the sacrificial agent DIPEA, forming an unstable peroxide anion B. Unstable intermediate B rearranges to form phenylboronic acid dihydrogen salt C. Finally, the intermediate C undergoes hydrolysis, yielding the final product, phenol.

1 S. Bhat, M. Aasif, M. Ahmad, F. Khurshaid, G. N. Yatoo, Z. K. Rather, G. A. Bhat, J. Banday, M. Wahid, *ACS Sustainable Chem. Eng.*, 2024, **12**, 141-153.

2. X. Dong, H. Hao, F. Zhang, X. Lang, *Appl. Catal. B-Environ.*, 2022, **309**, 121210.

Section S5. Tables S1-S4

Table S1. The total DFTB energies, and the crystal stacking energies per monolayer as well as the corresponding HOMO-LUMO energy gap for TpTfbPa-COF with directly and reverse stacked.

Stacking	***c* [Å]**	**Total DFTB Energy [a.u.]**	**Total crystal stacking energy [kcal mol–1]**	**HOMO-LUMO gap [eV]**
Monolayer		-95.863146		
AA	6.93	-191.800297	-23.22	2.023
AB	6.90	-191.754179	-8.75	2.149
Reversed-AA	6.87	-191.803152	-24.12	2.145

Table S2. Photocatalytic oxidation of phenylboronic acid to phenol.[a]

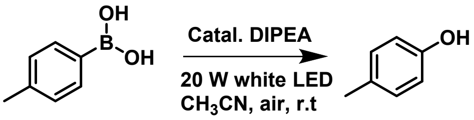

Entry	**Photocatalyst**	**Solvent**	**Time（h）**	**Yield(%)[b]**
1	Catalyst-free	CH_3CN	4	none
2	TfbTpPa-COF	CH_3CN	4	97
3	TfbTpPa-COF	Dioxane	4	60
4	TfbTpPa-COF	Ethanol	4	75
5	TfbTpPa-COF	CH_3CN	1	34
6	TfbTpPa-COF	CH_3CN	3	81
7[c]	TfbTpPa-COF	CH_3CN	4	97
8[d]	TfbTpPa-COF	CH_3CN	4	53
9	TpPa-COF	CH_3CN	4	70
10	TfbPa-COF	CH_3CN	4	98
11[e]	Mixture of TfbPa-COF and TpPa-COF	CH_3CN	4	33

[a]Reaction conditions: phenylboronic acid (0.25 mmol), COF (5 mg), DIPEA (1.25 equiv), white LEDs (20W), solvent (2 mL), air (1 atm), 4 h. [c]Using the DIPEA as the base. [d]Using the TEA as the base. [e]The dosage of COF is 5 mg (2.5 mg of TfbPa-COF and 2.5 mg of TpPa-COF). The yield was determined by ^1H NMR using 1,3,5-trimethoxybenzene as the internal standard.

Table S3. Coordinates for the reversible AA stacking structure of the TpTfbPa-COF.

atom	x	y	z
O1	0.28468	0.52770	0.25000
H2	0.51028	0.33353	0.25000
N3	0.58526	0.44042	0.25000
C4	0.68714	0.40297	0.25000
C5	0.61709	0.35384	0.25000
C6	0.56530	0.37541	0.25000
C7	0.53837	0.46460	0.25000
C8	0.56784	0.53636	0.25000
C9	0.46632	0.42381	0.25000
H10	0.62381	0.56839	0.25000
H11	0.44093	0.36773	0.25000
H12	0.70255	0.45755	0.25000
N13	0.41208	0.55316	0.25000
C14	0.30756	0.59167	0.25000
C15	0.38188	0.64117	0.25000
C16	0.43004	0.61999	0.25000
C17	0.45591	0.52600	0.25000
C18	0.42597	0.45412	0.25000
C19	0.52780	0.56698	0.25000
H20	0.36997	0.42194	0.25000
H21	0.55277	0.62300	0.25000
H22	0.35835	0.51942	0.25000
H23	0.48489	0.65931	0.25000
O24	0.47230	0.75698	0.25000
H25	0.66647	0.17675	0.25000
N26	0.55958	0.14484	0.25000
C27	0.59703	0.28418	0.25000
C28	0.64616	0.26326	0.25000
C29	0.62459	0.18990	0.25000
C30	0.53540	0.07377	0.25000
C31	0.46364	0.03148	0.25000
C32	0.57619	0.04252	0.25000
H33	0.43161	0.05542	0.25000
H34	0.63227	0.07320	0.25000
H35	0.54245	0.24500	0.25000
N36	0.44684	0.85892	0.25000
C37	0.40833	0.71589	0.25000
C38	0.35883	0.74071	0.25000
C39	0.38001	0.81005	0.25000

C40	0.47400	0.92991	0.25000
C41	0.54588	0.97186	0.25000
C42	0.43302	0.96081	0.25000
H43	0.57806	0.94803	0.25000
H44	0.37700	0.92977	0.25000
H45	0.48058	0.83893	0.25000
H46	0.34069	0.82558	0.25000
O47	0.24302	0.71532	0.25000
H48	0.82325	0.48972	0.25000
N49	0.85516	0.41474	0.25000
C50	0.71582	0.31286	0.25000
C51	0.73674	0.38291	0.25000
C52	0.81010	0.43470	0.25000
C53	0.92623	0.46163	0.25000
C54	0.96852	0.43216	0.25000
C55	0.95748	0.53368	0.25000
H56	0.94458	0.37619	0.25000
H57	0.92680	0.55907	0.25000
H58	0.75500	0.29745	0.25000
N59	0.14108	0.58792	0.25000
C60	0.28411	0.69244	0.25000
C61	0.25929	0.61812	0.25000
C62	0.18995	0.56996	0.25000
C63	0.07009	0.54409	0.25000
C64	0.02814	0.57403	0.25000
C65	0.03919	0.47220	0.25000
H66	0.05197	0.63003	0.25000
H67	0.07023	0.44723	0.25000
H68	0.16107	0.64165	0.25000
H69	0.17442	0.51511	0.25000
O70	0.71532	0.47230	0.75000
H71	0.48972	0.66647	0.75000
N72	0.41474	0.55958	0.75000
C73	0.31286	0.59703	0.75000
C74	0.38291	0.64616	0.75000
C75	0.43470	0.62459	0.75000
C76	0.46163	0.53540	0.75000
C77	0.43216	0.46364	0.75000
C78	0.53368	0.57619	0.75000
H79	0.37619	0.43161	0.75000
H80	0.55907	0.63227	0.75000
H81	0.29745	0.54245	0.75000
N82	0.58792	0.44684	0.75000

C83	0.69244	0.40833	0.75000
C84	0.61812	0.35883	0.75000
C85	0.56996	0.38001	0.75000
C86	0.54409	0.47400	0.75000
C87	0.57403	0.54588	0.75000
C88	0.47220	0.43302	0.75000
H89	0.63003	0.57806	0.75000
H90	0.44723	0.37700	0.75000
H91	0.64165	0.48058	0.75000
H92	0.51511	0.34069	0.75000
O93	0.52770	0.24302	0.75000
H94	0.33353	0.82325	0.75000
N95	0.44042	0.85516	0.75000
C96	0.40297	0.71582	0.75000
C97	0.35384	0.73674	0.75000
C98	0.37541	0.81010	0.75000
C99	0.46460	0.92623	0.75000
C100	0.53636	0.96852	0.75000
C101	0.42381	0.95748	0.75000
H102	0.56839	0.94458	0.75000
H103	0.36773	0.92680	0.75000
H104	0.45755	0.75500	0.75000
N105	0.55316	0.14108	0.75000
C106	0.59167	0.28411	0.75000
C107	0.64117	0.25929	0.75000
C108	0.61999	0.18995	0.75000
C109	0.52600	0.07009	0.75000
C110	0.45412	0.02814	0.75000
C111	0.56698	0.03919	0.75000
H112	0.42194	0.05197	0.75000
H113	0.62300	0.07023	0.75000
H114	0.51942	0.16107	0.75000
H115	0.65931	0.17442	0.75000
O116	0.75698	0.28468	0.75000
H117	0.17675	0.51028	0.75000
N118	0.14484	0.58526	0.75000
C119	0.28418	0.68714	0.75000
C120	0.26326	0.61709	0.75000
C121	0.18990	0.56530	0.75000
C122	0.07377	0.53837	0.75000
C123	0.03148	0.56784	0.75000
C124	0.04252	0.46632	0.75000
H125	0.05542	0.62381	0.75000

H126	0.07320	0.44093	0.75000
H127	0.24500	0.70255	0.75000
N128	0.85892	0.41208	0.75000
C129	0.71589	0.30756	0.75000
C130	0.74071	0.38188	0.75000
C131	0.81005	0.43004	0.75000
C132	0.92991	0.45591	0.75000
C133	0.97186	0.42597	0.75000
C134	0.96081	0.52780	0.75000
H135	0.94803	0.36997	0.75000
H136	0.92977	0.55277	0.75000
H137	0.83893	0.35835	0.75000
H138	0.82558	0.48489	0.75000

Table S4. Investigation of the photocatalytic oxidation of phenylboronic acid using various quenchers, and TpTfbPa-COF as the catalyst.[a]

Scavenger	**Species quenched**	**Yield(%)**
ETCR	h^+	40
AgNO3	e^-	12
p-BQ	O_2^-	8
blank	--	97
i-PrOH	$^{\bullet}$ $^{-}$OH	93

[a]Reaction conditions: phenylboronic acid (0.25 mmol), COF (5 mg), DIPEA (1.25 equiv), white LEDs (20W), solvent (2 mL), air (1 atm), 4 h. The yield was determined by ^{1}H NMR using 1,3,5-trimethoxybenzene as the internal standard.